Polymer 50 (2009) 6049–6056

Contents lists available at ScienceDirect

Polymer

journal homepage: www.elsevier.com/locate/polymer

Toluene and *n*-heptane sorption in Matrimid® asymmetric hollow fiber membranes

Jong Suk Lee, Ryan T. Adams, William Madden, William J. Koros*

School of Chemical and Biomolecular Engineering, Georgia Institute of Technology, Atlanta, GA-30332, USA

ARTICLE INFO

Article history:
Received 11 July 2009
Received in revised form
3 October 2009
Accepted 7 October 2009
Available online 31 October 2009

Keywords:
Sorption
n-heptane
Toluene

ABSTRACT

Equilibrium and transient sorption isotherms were obtained for toluene and *n*-heptane in both annealed and non-annealed Matrimid® asymmetric hollow fiber membranes at 35 °C. Equilibrium sorption follows the dual mode model except for toluene sorption into annealed fibers above a pressure of 0.5 psia. Except at the highest toluene exposure pressure, the equilibrium uptake of penetrant in annealed fibers was signigicantly less than in non-annealed fibers at a given pressure due to the significant reduction of excess free volume. Changes in the dual mode model parameters for the annealed samples may reflect not only reductions in sample free volume, but also charge transfer formation. The Berens–Hopfenberg model successfully describes all of the various transient sorption behaviors observed for toluene and *n*-heptane in Matrimid® with a significant relaxation-controlled contribution to the overall mass uptake over much of the experimental range explored. Purely diffusion-controlled (Fickian) uptake was seen only for toluene sorption in annealed fibers for a change in activity from 0 to 0.05, while purely relaxation-controlled (non-Fickian) uptake was observed for *n*-heptane sorption in non-annealed fibers for a change in activity from 0 to 0.09. A reduced value of D_A/L^2, the effective Fickian diffusion time, in non-annealed fibers for toluene at a low activity level provides evidence of antiplasticization, while at intermediate to high activity, the value of D_A/L^2 increases with activity for all of the systems studied in this work indicating plasticization.

1. Introduction

There are few reports on explored the effect of condensable aromatic and heavier aliphatic contaminants on membrane performance for gas separation [1–4]. The impact of these highly sorbing contaminants on the membrane system has still remained poorly understood due to the complexity of these components and the difficulty in characterizing their effects experimentally.

This work investigates the transport properties of model aromatic and paraffin hydrocarbons using toluene and *n*-heptane in asymmetric Matrimid® hollow fiber membranes. Equilibrium and transient sorption isotherms are reported for both annealed and non-annealed fibers to investigate effects of annealing on toluene and *n*-heptane sorption and transport properties. Understanding the interactions of these condensable hydrocarbon contaminants with glassy asymmetric membranes is useful for analyzing state of the art membranes for natural gas feeds containing aromatic and aliphatic contaminants. This study, therefore, provides a basis for subsequent studies regarding ternary and quaternary feed mixture of CO_2, CH_4, with one or more of these components as model hydrocarbon contaminants found in natural gas. The focus of the subsequent studies [5,6] is on the CO_2 and CH_4 transport behavior of the same asymmetric membranes discussed here. The current study considers the simpler case without CO_2 or CH_4 components. Working with these simpler feeds allows understanding the changes induced in the glassy polymer matrix by these heavy hydrocarbon sorbates.

2. Experimental

2.1. Materials

The membranes studied in this work were all formed from Matrimid® 5218 a wholly amorphous polyimide that is manufactured and marketed by Huntsman LLC. The backbone repeat structure of Matrimid® is shown in Fig. 1, and Table 1 provides physical properties for Matrimid®. Matrimid® hollow fibers are spun using a dry-jet/wet-quench process [7–10] using a polymer dope consisting of Matrimid®, *N*-methyl pyrrolidinone acting as a solvent, and ethanol acting as a non-solvent. A skin thickness of defect-free Matrimid® fibers is approximately 100 nm. The nodular

* Corresponding author. Tel.: +404 385 2845; fax: +404 385 2683.
E-mail address: wkoros@chbe.gatech.edu (W.J. Koros).

0032-3861/$ – see front matter © 2009 Elsevier Ltd. All rights reserved.
doi:10.1016/j.polymer.2009.10.015

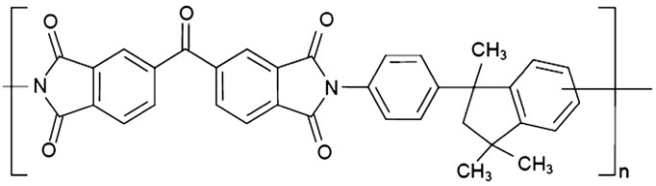

Fig. 1. Matrimid® repeat structure.

or porous support layer of the fiber has characteristic dimensions of the same order of magnitude. A scanning electron micrograph illustrates the asymmetric hollow fiber morphology in Fig. 2. For the annealed sample preparation, fibers were annealed at 220 °C for 12–16 h under vacuum.

2.2. Gravimetric vapor sorption

The McBain quartz spring method is used to measure sorption gravimetrically of highly sorbing vapors [11–13]. A sample is hung on a calibrated quartz spring (Ruska Instruments) with a spring constant of 2.51×10^{-3} g/cm. Both sample and quartz spring are located in a glass chamber maintained at 35 °C by a hot water jacket. The rest of the system is heated to prevent condensation of the vapor on the side walls. The pressure in a glass chamber is measured using a MKS Baratron® 1000 torr pressure transducer (Type 727). Typical polymer sample weights in this work are approximately 25 mg.

The sample is loaded and completely degassed before each sorption experiment is performed. In order to remove all air in the headspace of the liquid vial and dissolved gases, at least five freeze-pump-thaw cycles were performed prior to each sorption experiment. For the equilibrium sorption experiment, equilibrium is assumed to be attained when the spring position does not change over the course of 24 h. As for kinetic sorption, more frequent data collection was performed to obtain a more accurate diffusion coefficient at each activity level. The extension of the spring can be measured to within 5 μm using the cathetometer. Once equilibrium is confirmed, more vapor is introduced for the next activity level of sorption measurement. The concentration of vapors sorbed in the polymer, ccSTP/cc polymer, is calculated by Equation (1).

$$C = (K\Delta x)\left(\frac{22,414 \times \rho_p}{M_w \times M_p}\right) \quad (1)$$

K is the spring constant, g/cm, $\triangle x$ is the change in spring position, cm, ρ_p is the polymer density, g/cc, M_w is the molecular weight of highly sorbing vapors (i.e. 92.1 g/mol for toluene and 100.2 g/mol for *n*-heptane), and M_p is the mass of the polymer sample, g.

3. Results and discussion

3.1. Equilibrium sorption of n-heptane and toluene

Equilibrium sorption experiments of *n*-heptane and toluene were performed at 35 °C in small steps of increasing pressure. The dual mode sorption and transport model describes sorption, diffusion, and permeation of penetrants in glassy polymers [14]. This idealized model considers, two types of microscopic sorption populations comprising sorption in unrelaxed (non-equilibrium) volume regions (C_H) and the densely packed (equilibrium) volume regions (C_D), respectively. Penetrant in these two populations are assumed to be in local equilibrium with each other. The basis for this model is the known fact that cooling an amorphous polymer below its glass transition temperature locks in intersegmental molecular scale packing defects or excess free volume, sometimes referred to as "holes". On the other hand, densely packed region representative of more or less equilibrium sorption sites are envisioned to comprise zones of well packed segment, in which penetrant sorbs in a "dissolved" mode (C_D) similar to that in a simple rubbery polymer or liquid. Combining these regions leads to the dual mode sorption expression in equation (2).

$$C = \frac{C'_H bp}{1 + bp} + k_D p \quad (2)$$

The first term represents Langmuir type sorption in the non-equilibrium regions and the second term represents Henry's law sorption in the equilibrium region. C_H' is the Langmuir capacity constant, ccSTP/ cc polymer, and b is Langmuir affinity constant, $psia^{-1}$, p is the pressure of penetrants in equilibrium with the polymer. The k_D parameter is the Henry's law solubility coefficient, ccSTP/ cc polymer/psia.

The sorption isotherms of *n*-heptane in both annealed and non-annealed Matrimid® asymmetric hollow fibers are shown in Fig. 3. As shown in Fig. 3, both isotherms are well described by the dual mode model of sorption in glassy polymers up to an activity level of 0.7. Also, the *n*-heptane sorption capacity in the annealed fiber samples is substantially lower than that in non-annealed fibers. The corresponding dual mode parameters for *n*-heptane are given in Table 2. It is surprising that annealing causes a substantial increase in Langmuir affinity constant, b.

The equilibrium sorption isotherms for toluene in both non-annealed and annealed fibers are given in Fig. 4. As observed previously for *n*-heptane, the toluene sorption capacity of the annealed fiber sample is substantially lower than that of the non-annealed sample. Moreover, the isotherm of annealed fiber above 0.5 psia shows an upward inflection that the dual mode model is not capable of capturing. At these relatively high pressures, the sorption of toluene in annealed fibers approaches that of non-annealed fibers. Zhou saw a similar behavior for the sorption of acetic acid at high activity in Matrimid® asymmetric hollow fiber membranes [15]. Apparently, the effect of annealing is lost in the presence of high activities of toluene (See dotted line in Fig. 4) and it is believed that high activity level of toluene overcomes the effects of annealing, while the lower sorbing *n*-heptane is not able to do so. It should be noted that this effect with toluene occurs at a much higher sorption level than that achieved with *n*-heptane. It can be hypothesized that the effect of annealing may be lost with any penetrant capable of achieving a critical sorption level. The dual mode parameters for toluene are given in Table 3. As with *n*-heptane, annealing of the fiber sample generates a substantial reduction in the Langmuir capacity constant, C_H', and an increase in the Langmuir affinity constant, b. It is interesting that annealing increases the Henry's law constant, k_D, unlike *n*-heptane.

From examination of Table 2 and Table 3, it is apparent that the effect of annealing on the dual mode model parameters is generally similar, but not identical for both *n*-heptane and toluene. For both penetrants, the value of the Langmuir capacity constant, C_H', decreases and the value of the Langmuir affinity constant, b, increases due to annealing. Unlike *n*-heptane, for which the value of the Henry's Law constant, k_D, remains approximately constant as

Table 1
Physical properties of Matrimid® material at 65 psia and 35 °C [7].

T_g	305 [°C]
Density	1.2 [g/cm^3]

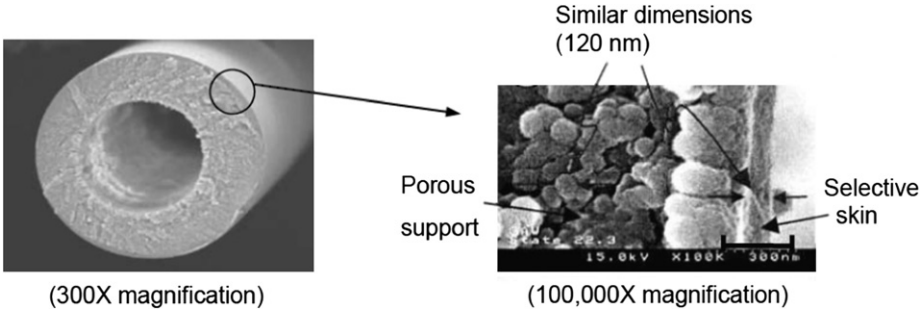

Fig. 2. SEM images of 280 μm outer diameter Matrimid® hollow fibers. Characteristic dimensions of the nodular, porous support layer are similar in size to the skin thickness [9].

expected, k_D for toluene increases due to annealing. It is surprising that annealing results in an increase in b and k_D, since past studies of annealing and physical aging showed primarily a simple reduction in C_H', while values of k_D and b remained relatively unaffected [16–18]. Typically, sub-T_g thermal annealing is thought to simply accelerate the rate of physical aging, or the rate of volume reduction [19–21]. If this assumption holds, only reductions in C_H' would be observed from annealing; however, annealing of Matrimid® asymmetric hollow fibers also results in increased values of k_D and b. In this work, the observed increases in k_D and b due to annealing may be related to charge transfer complex formation. In earlier work, Fourier Transform Infrared Spectroscopy (FTIR) showed that the spectra of the untreated and treated Matrimid fibers are almost identical, demonstrating that heat treatment does not cause any chemical crosslinking [15]. UV fluorescence spectroscopy suggested the formation of charge transfer complexes after annealing. Since our work used the same source materials and annealing protocol, similar charge transfer complexing is expected. The formation of such charge transfer complexes could essentially create a sufficiently new material with the same chemical structure but different inter and intra-chain interactions and packing to affect the values of k_D and b. Added mobility at high temperature from thermal annealing can enable the formation of charge transfer complexes as well as relax excess glassy state volume. While speculative, this suggestion could indicate avenues for using other probe molecules with similar size and shape, but with different polarities, e.g., chlorobenzene or phenol vs. toluene and 1-chlorohexane or 1-hexanol vs. heptane. Such future studies could determine if similar or larger changes in affinity constants are observed for these more complex cases. In any case, the reduction in C_H' due to annealing exceeds the increases observed in k_D and b, thereby resulting in the lower equilibrium uptake of penetrant in the annealed samples. This trend would be expected even for more polar penetrants as well. The value of C_H' is often correlated with the excess fractional free volume of polymer as [22–25]:

$$C_H' = \left(\frac{V_g - V_l}{V_g}\right)\rho^* \tag{3}$$

where, V_g is the specific volume of the polymer in the glassy state, V_l is the specific volume of the polymer in a hypothetical liquid state, and ρ^* is the liquid-like molar density of the penetrant in the Langmuir region. The significant reductions in sorption for both penetrants due to annealing, therefore, primarily represent a significant reduction in the free volume of the fibers.

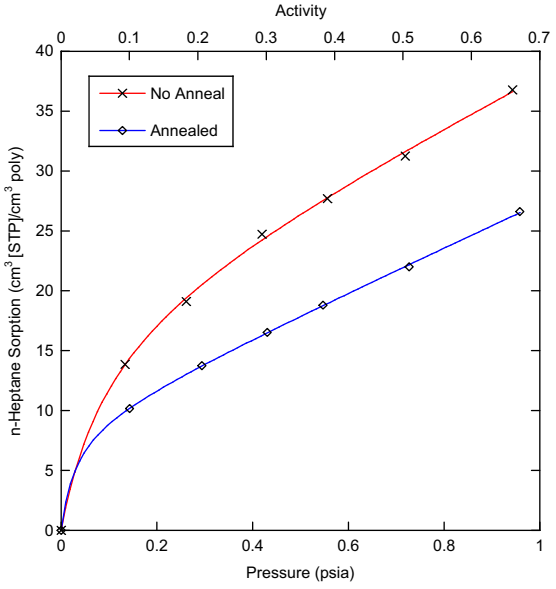

Fig. 3. Sorption isotherm of n-heptane in both annealed (open diamond) and non-annealed (cross) fibers at 35 °C (Solid lines are fit to dual mode model).

3.2. Transient sorption of n-heptane and toluene

The time-dependent uptake of gas/vapor into a glassy polymer exhibits many possible behaviors [26–31]. The simplest of these behaviors is Fickian diffusion-controlled uptake of gas into the glassy polymer matrix. In this case, the time-dependent uptake into a sheet of thickness L can be determined by solving the diffusion equation with constant boundary conditions and uniform initial concentration of penetrant in the polymer. Crank [32] gives a solution for this case:

$$\left(\frac{M_t}{M_\infty}\right) = 1 - \sum_{n=0}^{\infty} \frac{8}{\pi^2(2n+1)^2} \exp\left(\frac{-D_A(2n+1)^2\pi^2 t}{L^2}\right) \tag{4}$$

where D_A is the diffusion coefficient of gas 'A' in the polymer, and M_t and M_∞ are the masses of the penetrant sorbed at times t and ∞. The mathematics of Fickian diffusion are often complicated by the highly concentration dependent diffusion coefficients which occur in glassy polymers; however, one can still fit the kinetic response if

Table 2
Dual mode model parameters for n-heptane sorption in Matrimid® asymmetric hollow fibers at 35 °C.

Fiber Sample	$k_D\left(\frac{ccSTP}{ccPoly \cdot psia}\right)$	$C_H'\left(\frac{ccSTP}{ccPoly}\right)$	$b\left(\frac{1}{psia}\right)$
Non-Annealed	19.9 ± 1.6	19.8 ± 1.8	9.7 ± 2.1
Annealed	18.4 ± 0.4	9.2 ± 0.3	32.2 ± 7.1

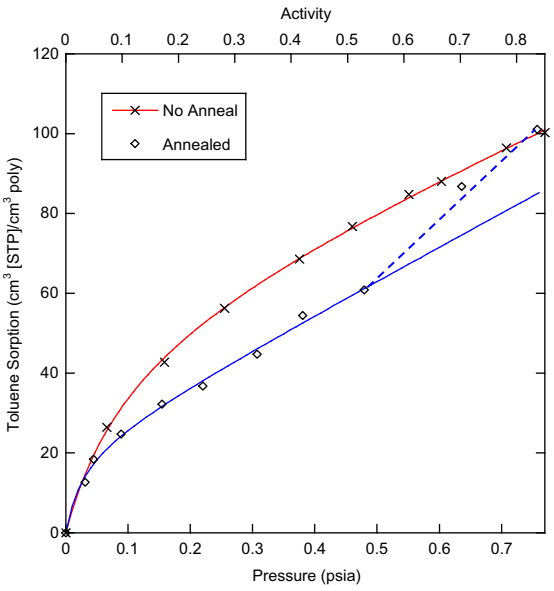

Fig. 4. Sorption isotherm of toluene in both annealed (open diamond) and non-annealed (cross) fibers at 35 °C (Solid lines are fit to dual mode model. Dotted lines shown is to aid the eye and is not theoretically predicted).

D_A is interpreted as an average coefficient applicable over the applicable concentration range.

In addition to the added complexity of concentration dependent diffusion, glassy polymers can also experience relaxation-controlled uptake of penetrant. As penetrant sorbs into the polymer matrix, the segmental mobility of polymer chains may increase in a delayed manner, thereby allowing for relaxation. As the polymer matrix relaxes, more room becomes available for penetration occupation. The time-scale of these relaxation processes is usually much longer than that of diffusion. Berens and Hopfenberg [33] proposed a model to account for the simultaneous processes of Fickian and relaxation driven uptake occurring in glassy polymers. In this model the mass uptake M_t is given as:

$$\left(\frac{M_t}{M_\infty}\right) = \left[(1-\alpha_R)\left\{1-\sum_{n=0}^{\infty}\frac{8}{(2n+1)^2}\exp\left(\frac{-D_A(2n+1)^2\pi^2 t}{L^2}\right)\right\}\right] + \left[\alpha_R\left\{1-\exp\left(\frac{-t}{\tau_R}\right)\right\}\right] \quad (5)$$

where α_R is the fraction of mass uptake occurring via a relaxation-controlled process, $(1-\alpha_R)$ is the fraction of mass uptake occurring via a diffusion-controlled, and τ_R is the time constant of the relaxation process. Although the Berens–Hopefenberg model accounts for the simultaneous occurrence of diffusion-controlled and relaxation-controlled uptake; it is often possible to divide the mass uptake into two distinct stages where the initial, fast uptake is associated with the Fickian response and the longer, slower approach to equilibrium is controlled by the relaxation process.

Table 3
Dual mode model parameters for toluene sorption in Matrimid® asymmetric hollow fibers at 35 °C.

Fiber Sample	$k_D\left(\frac{ccSTP}{ccPoly\cdot psia}\right)$	$C'_H\left(\frac{ccSTP}{ccPoly}\right)$	$b\left(\frac{1}{psia}\right)$
Non-Annealed	67.7 ± 3.5	55.8 ± 3.5	9.3 ± 1.1
Annealed	83.9 ± 7.4	22.2 ± 3.4	34.7 ± 14.5

Transient sorption isotherms were collected at 35 °C for toluene and *n*-heptane in non-annealed and annealed Matrimid® asymmetric hollow fiber membranes. Four types of isotherms are observed. Purely Fickian uptake is seen only for toluene sorption in annealed fibers for a change in activity from 0 to 0.05 and is shown in Fig. 5. As shown in Fig. 5, uptake of toluene in annealed fibers at an activity of 0.05 procedes via a purely diffusion-controlled process. In this case, a Fickian diffusion coefficient of 1.1×10^{-11} cm^2/sec may be calculated by assuming a characteristic thickness of 120 nm for the typical morphological features of the asymmetric hollow fiber membranes illustrated in Fig. 2. This value of the diffusion coefficient is reasonable based on previous investigations of solvent transport in other polymers [34–36]. Nevertheless, this calculation of the diffusion coefficient is only approximate, since the characteristic thickness of 120 nm was estimated by simple inspection of the morphology in Fig. 2. Although the value of 120 nm is an estimate, the observation of Fickian uptake in Matrimid® asymmetric hollow fibers indicates that a single characteristic thickness does exist for this morphology. Zimmerman et al. showed that in morphologies where a distribution exists in the characteristic dimension, apparent Fickian uptake, such as that shown in Fig. 5, will not be observed [37]. However, the fact that such a well-behaved Fickian response is observed strongly suggests that a well-defined characteristic dimension does exist within this complex asymmetric hollow fiber morphology.

On the other hand, purely relaxation-controlled uptake was observed for *n*-heptane sorption in non-annealed fibers for a change in activity from 0 to 0.09, and this behavior is shown in Fig. 6. The presence of its total chain relaxation-controlled kinetics at low activity verifies that n-heptane is a highly sorbing penetrant able to increase segmental motion associated with chain relaxation.

The majority of the transient sorption isotherms observed showed some amount of simultaneous diffusion-controlled (i.e. Fickian) uptake and relaxation-controlled uptake. Transient isotherms which show uptake by both mechanisms are of two distinct types. The first type is a smooth, concave-down curve gradually approaching the final equilibrium uptake. Fig. 7 shows this behavior for *n*-heptane sorption in non-annealed fibers from

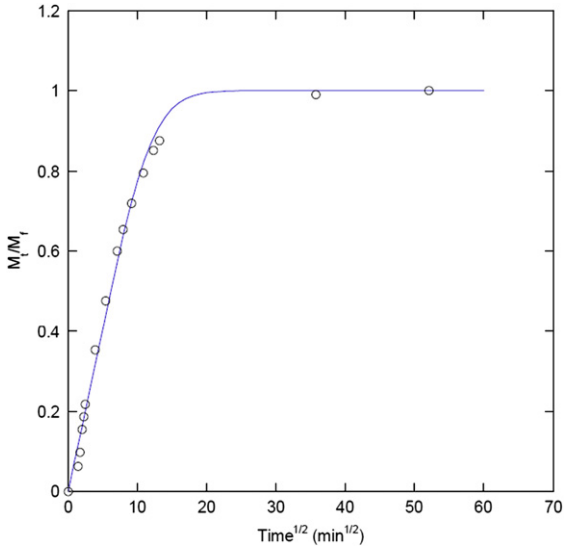

Fig. 5. Example of diffusion-controlled Fickian uptake for toluene sorption in annealed Matrimid® asymmetric hollow fiber membranes from an activity change of 0.0 to 0.05 at 35 °C. Solid line is Berens–Hopfenberg model fit with $\alpha_R = 0$, $D_A/L^2 = 1.3\times10^{-3}$ sec^{-1}, and $\tau_R = 0$ min.

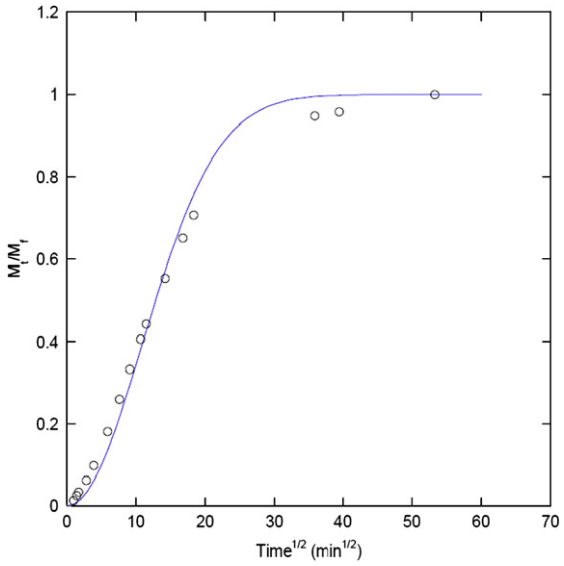

Fig. 6. Example of relaxation-controlled uptake for *n*-heptane sorption in non-annealed Matrimid® asymmetric hollow fiber membranes from an activity change of 0.0 to 0.09 at 35 °C. Solid line is Berens–Hopfenberg model fit with $\alpha_R = 1$, $D_A/L^2 = 0$ sec^{-1}, and $\tau_R = 238$ min.

a 0.09 to 0.18 step in activity. The second type of transient isotherm more clearly showed vapor uptake by both diffusion and relaxation-controlled processes. In these so-called "two-stage" transient sorption isotherms, an initial quick diffusion-controlled, Fickian uptake is followed by a longer relaxation-controlled uptake [38,39]. This behavior is show in Fig. 8 for toluene sorption in non-annealed fibers from a 0.51 to 0.61 activity step.

The Berens–Hopfenberg model parameters are given for toluene and *n*-heptane sorption in annealed and non-annealed Matrimid® asymmetric hollow fiber membranes for all activities tested in this work in Figs. 9–12. The Berens–Hopfenberg model fit all of the data remarkably well; however, interpretation of the model parameters is complex. The effect of penetrant activity and thermal history on the Berens–Hopfenberg parameters will be described with an interpretation of these results. Berens–Hopfenberg parameter

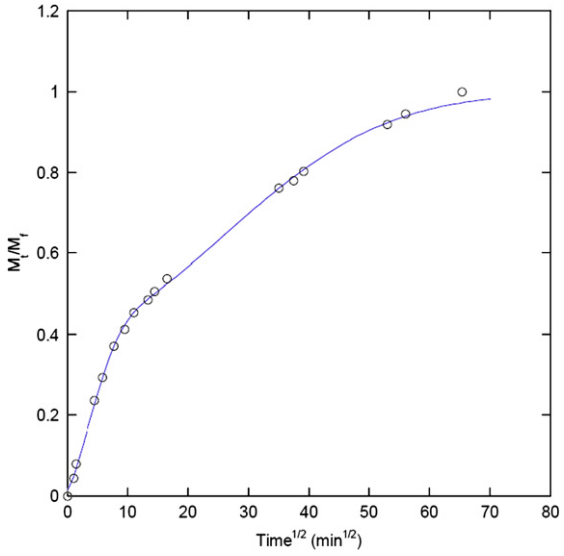

Fig. 7. Example of simultaneous diffusion and relaxation-controlled uptake for *n*-heptane sorption in non-annealed Matrimid® asymmetric hollow fiber membranes from an activity change of 0.09 to 0.18 at 35 °C. Solid line is Berens–Hopfenberg model fit with $\alpha_R = 0.58$, $D_A/L^2 = 2.5\times10^{-3}$ sec^{-1}, and $\tau_R = 1391$ min.

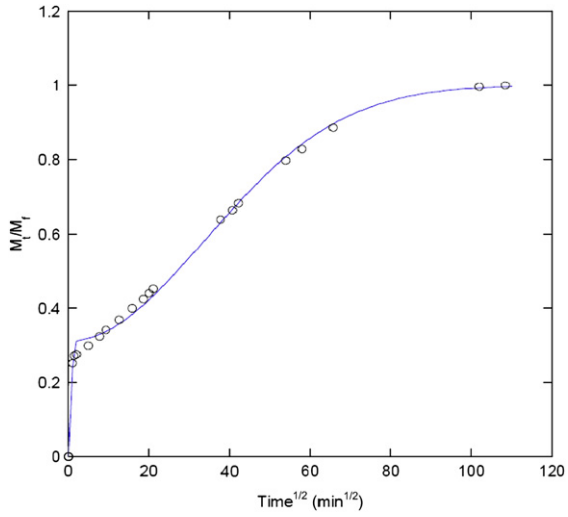

Fig. 8. Example of "two-stage" uptake for toluene sorption in non-annealed Matrimid® asymmetric hollow fiber membranes from an activity change of 0.51 to 0.61 at 35 °C. Solid line is Berens–Hopfenberg model fit with $\alpha_R = 0.69$, $D_A/L^2 = 1.3\times10^{-1}$ sec^{-1}, and $\tau_R = 2285$ min.

trends for *n*-heptane sorption in non-annealed samples are given in Fig. 9. As shown, the value of diffusional resistance, $1/(D_A/L^2)$, generally decreases with an increasing activity level of *n*-heptane after the first activity step, where the total chain relaxation-

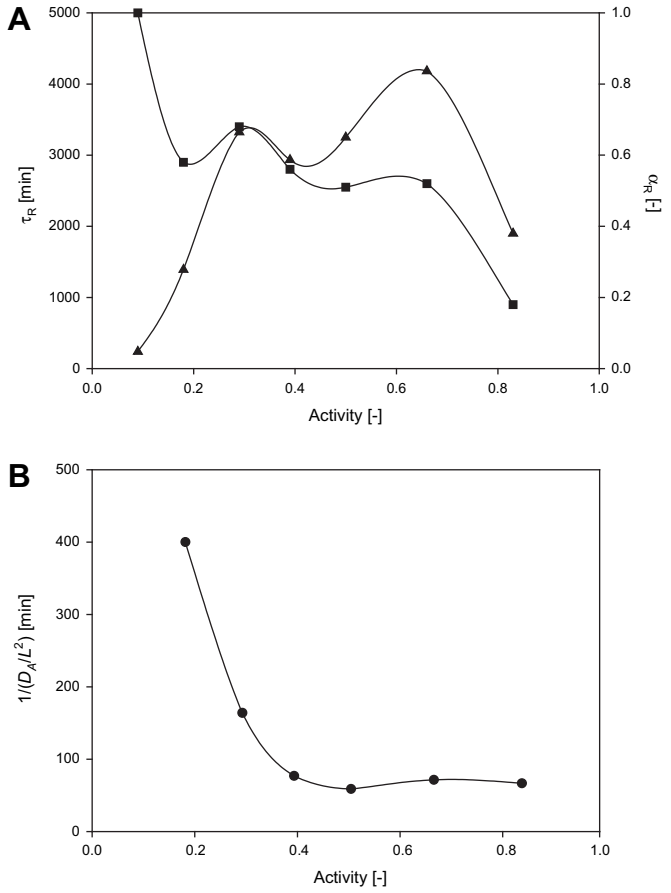

Fig. 9. Berens–Hopfenberg model parameters for *n*-heptane sorption in non-annealed Matrimid® asymmetric hollow fiber membranes at 35 °C (In (A), black triangle-relaxation resistance: τ_R, black rectangular-fractional resistance: α_R; In (B), black circle-diffusional resistance: $1/(D_A/L^2)$. The lines shown are to aid the eye and are not theoretically predicted).

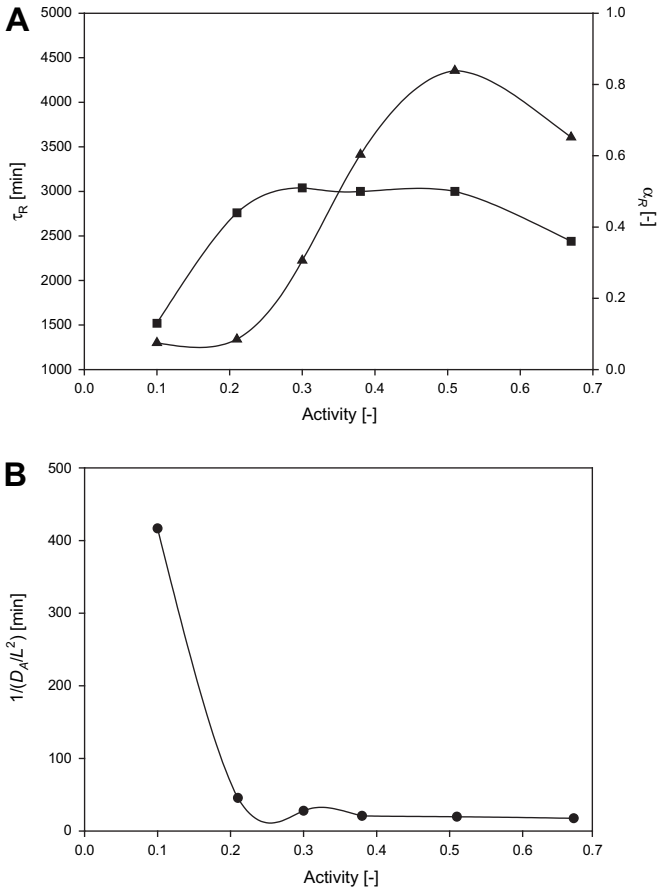

Fig. 10. Berens–Hopfenberg model parameters for *n*-heptane sorption in annealed Matrimid® asymmetric hollow fiber membranes at 35 °C (In (A), black triangle-relaxation resistance: τ_R, black rectangular-fractional resistance: α_R; In (B), black circle-diffusional resistance: $1/(D_A/L^2)$. The lines shown are to aid the eye and are not theoretically predicted).

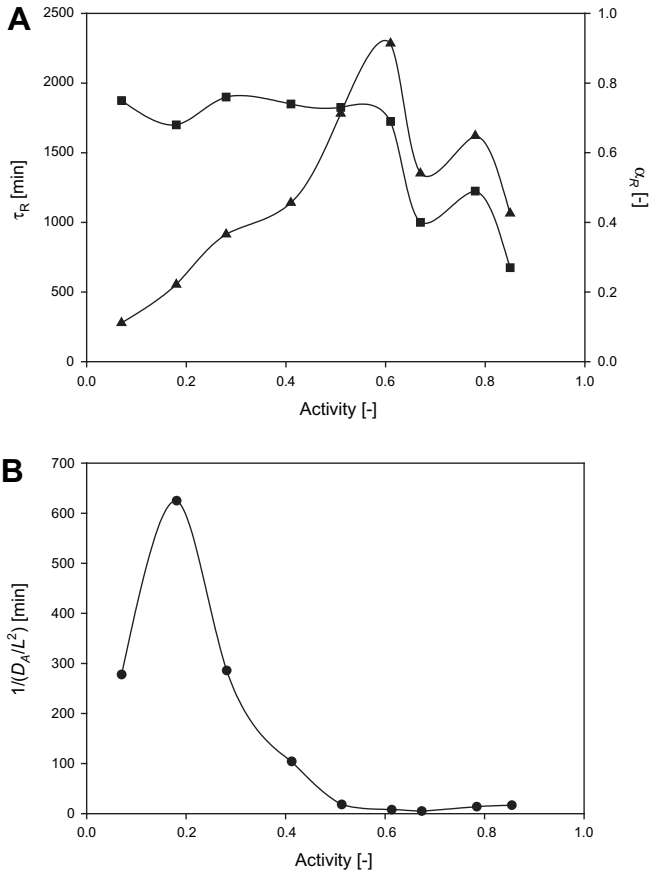

Fig. 11. Berens–Hopfenberg model parameters for toluene sorption in non-annealed Matrimid® asymmetric hollow fiber membranes at 35 °C (In (A), black triangle-relaxation resistance: τ_R, black rectangular-fractional resistance: α_R; In (B), black circle-diffusion resistance: $1/(D_A/L^2)$. The lines shown are to aid the eye and are not theoretically predicted).

controlled kinetics are observed. The "*L*" in Fig. 9 refers to the characteristic morphological feature, noted above to be reasonably estimated as 120 nm. The presence of its total chain relaxation-controlled kinetics at low activity verifies that *n*-heptane is a highly sorbing penetrant as discussed before. Moreover, an overall decrease in diffusional resistance is expected as increasing sorbed concentration should lead to higher chain mobility.

Berens–Hopfenberg parameter trends for *n*-heptane sorption in annealed samples are given in Fig. 10. Annealing fibers results in reduced magnitude of α_R across the full activity range compared to that of non-annealed suggesting that it hinders chain relaxation movement due to the reduction of excess free volume. This trend is consistent with a reduced sorption uptake of *n*-heptane in annealed fibers in equilibrium sorption due to a huge reduction in C'_H.

Berens–Hopfenberg parameter trends for toluene sorption in non-annealed samples are given in Fig. 11. All transient sorption isotherms for toluene in Matrimid® fibers show a significant relaxation-controlled contribution to the overall mass uptake based on the fact that its overall α_R values are relatively large. As with *n*-heptane sorption in non-annealed samples, the value of diffusional resistance, $1/(D_A/L^2)$, generally decreases with an increasing activity level of toluene. The decrease in diffusional resistance appears to be larger and more rapid compared to *n*-heptane, which is consistent with higher sorbed toluene concentration at a given activity as shown in equilibrium sorption isotherms. Furthermore, a larger value of α_R and a smaller value of τ_R for toluene in non-annealed fibers compared to the corresponding values for *n*-heptane support the suggestion that toluene is a more effective plasticizer than *n*-heptane. Again, it is consistent with sorption isotherms where toluene shows higher sorbed concentration at a given activity. Evidence of antiplasticization exists from the first two points of $1/(D_A/L^2)$, where its value increases. Antiplasticization of the polymer is known to result from sorption of some penetrants at low concentration. In the antiplasticization regime, sorbed penetrant hinders polymer segmental motion and thereby decreases the diffusion coefficient and possibly the chain relaxation rate responsible for relaxation-controlled uptake. On the other hand, at intermediate to high penetrant activity, plasticization of the polymer occurs, based on the fact that the value of $1/(D_A/L^2)$ decreases. In the plasticization regime, sorbed penetrant facilitates polymer segmental motion and, thereby, increases the diffusion coefficient of the sorbed penetrant. A drastic drop of values in τ_R at high activity further supports the idea that toluene plasticizes fibers strongly at high activity.

Lastly, Berens–Hopfenberg parameter trends for toluene sorption in annealed samples are given in Fig. 12. As shown in *n*-heptane case, annealing fibers reduces the magnitude of α_R values in the overall activity level compared to that of non-annealed, which is consistent with the reduced sorption uptake of annealed sample in sorption isotherms. Unlike the non-annealed sample, there is no discernible evidence of antiplasticization at low activity in annealed fiber. However, antiplasticization may still occur at activities lower than the lowest activity tested, based on

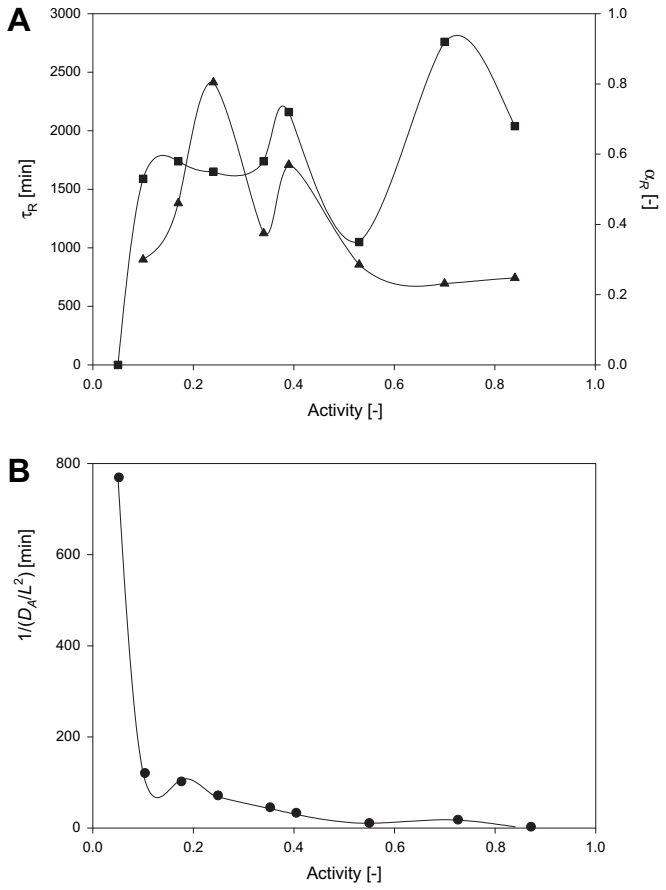

Fig. 12. Berens–Hopfenberg model parameters for toluene sorption in annealed Matrimid® asymmetric hollow fiber membranes at 35 °C (In (A), black triangle-relaxation resistance: τ_R, black rectangular-fractional resistance: α_R; In (B), black circle-diffusion resistance: $1/(D_A/L^2)$. The lines shown are to aid the eye and are not theoretically predicted).

the fact that annealing reduces excess free volume, thereby, decreasing the chain mobility.

4. Conclusions

The equilibrium sorption isotherms for toluene and *n*-heptane, in both annealed and non-annealed membranes, were well described by the dual mode sorption model. Thermal annealing of the fibers resulted in a significant decrease in the equilibrium sorption of all penetrants. Within the framework of the dual mode sorption model, the reduction in equilibrium sorption upon thermal annealing was correlated to a reduction of the Langmuir capacity constant, C_H'. The increases of k_D and b values in the dual mode model for the annealed samples are believed to be due to the formation of charge transfer complexes, which fundamentally alters the nature of the glassy matrix. All transient sorption isotherms of toluene and *n*-heptane in both annealed and non-annealed Matrimid® asymmetric hollow fiber membranes were well described by the Berens–Hopfenberg model. The range of transient sorption behaviors observed in this study was exceedingly complex. This complexity results from the interaction of concentration dependent phenomena such as antiplasticization/plasticization and history dependent phenomena such as the formation of charge transfer complexes.

Acknowledgements

The authors would like to acknowledge financial support from The Coca Cola Company, Air Liquide, and NSF for this research.

References

[1] Al-Juaied M, Koros WJ. Performance of natural gas membranes in the presence of heavy hydrocarbons. Journal of Membrane Science 2006;274(1–2):227–43.
[2] White LS, Blinka TA, Kloczewski HA, Wang IF. Properties of a polyimide gas separation membrane in natural-gas streams. Journal of Membrane Science 1995;103(1-2):73–82.
[3] Pereira B, Admassu W. Effects of chemical impurities on gas sorption in polymeric membranes. I. polycarbonate and polysulfone. Separation Science and Technology 2001;36(2):177–97.
[4] Pereira B, Admassu W, Jensvold J. Effects of chemical impurities on gas sorption in polymeric membranes. II. PC-1 and PC-2. Separation Science and Technology 2001;36(3):417–42.
[5] Lee JS, Madden W, Koros WJ. Antiplasticization and plasticization of matrimid® asymmetric hollow fiber membranes- part A: experimental, submitted in Journal of Membrane Science, 2009.
[6] Lee JS, Madden W, Koros WJ. Antiplasticization and plasticization of matrimid® asymmetric hollow fiber membranes- part B: modeling, submitted in Journal of Membrane Science, 2009.
[7] Moore T. Effects of materials, processing, and operating conditions on the morphology and gas transport properties of mixed matrix membranes, in chemical engineering. Austin: The University of Texas; 2004.
[8] Clausi DT, Koros WJ. Formation of defect-free polyimide hollow fiber membranes for gas separations. Journal of Membrane Science 2000;167(1):79–89.
[9] Carruthers SB, Ramos GL, Koros WJ. Morphology of integral-skin layers in hollow-fiber gas-separation membranes. Journal of Applied Polymer Science 2003;90(2):399–411.
[10] Pinnau I, Koros WJ. Structures and gas separation properties of asymmetric polysulfone membranes made by dry, wet, and dry wet phase inversion. Journal of Applied Polymer Science 1991;43(8):1491–502.
[11] McBain JW, Lucas HP, Chapman PF. The sorption of organic vapors by highly evacuated, activated sugar charcoal. Journal of the American Chemical Society 1930;52:2668–81.
[12] McBain JW, Bakr AM. A new sorption balance. Journal of the American Chemical Society 1926;48(1):690–5.
[13] Jacques CHM, Hb Hopfenbe. Vapor and liquid equilibria in glassy polyblends of polystyrene and poly(2,6-dimethyl-1,4-phenylene oxide).I. Polymer Engineering and Science 1974;14(6):441–8.
[14] Koros WJ, Chan AH, Paul DR. Sorption and transport of various gases in polycarbonate. Journal of Membrane Science 1977;2(2):165–90.
[15] Zhou FB, Koros WJ. Pervaporation using hollow-fiber membranes for dehydrating acetic acid and water mixtures. Industrial & Engineering Chemistry Research 2006;45(5):1787–96.
[16] Stewart ME, Hopfenberg HB, Koros WJ. Characterization of physical aging of poly(methyl methacrylate) powders by a novel high-pressure sorption technique. Journal of Applied Polymer Science 1989;38(6):1111–26.
[17] Hachisuka H, Tsujita Y, Takizawa A, Kinoshita T. Gas-transport properties of annealed polyimide films. Journal of Polymer Science, Part B:Polymer Physics 1991;29(1):11–6.
[18] Mohamed HFM, El-Sayed AMA, Abdel-Hady EE. Study of sorption in poly(vinyl alcohol) using the positron annihilation technique. Journal of Physics-Condensed Matter 1999;11(22):4461–7.
[19] Fuhrman C, Nutt M, Vichtovonga K, Coleman MR. Effect of thermal hysteresis on the gas permeation properties of 6FDA-based polyimides. Journal of Applied Polymer Science 2004;91(2):1174–82.
[20] Ho CH, Vu-Khanh T. Effects of time and temperature on physical aging of polycarbonate. Theoretical and Applied Fracture Mechanics 2003;39(2):107–16.
[21] Wang Y, Shen DY, Qian RY. Subglass-transition-temperature annealing of poly(ethylene terephthalate) studied by FTIR. Journal of Polymer Science, Part B:Polymer Physics 1998;36(5):783–8.
[22] Wonders AG, Paul DR. Effect of CO_2 exposure history on sorption and transport in polycarbonate. Journal of Membrane Science 1979;5(1):63–75.
[23] Koros WJ, Paul DR. CO_2 sorption in poly(ethylene-terephthalate) above and below glass-transition. Journal of Polymer Science, Part B:Polymer Physics 1978;16(11):1947–63.
[24] Koros WJ, Paul DR. Sorption and transport of CO_2 in poly(ethylene-terephthalate) above and below T_g. Organic Coatings and Plastic Chemistry 1978;39:172–7.
[25] Kanehashi S, Nagai K. Analysis of dual-mode model parameters for gas sorption in glassy polymers. Journal of Membrane Science 2005;253(1–2):117–38.
[26] Frisch HL, Stern SA. Diffusion of small molecules in polymers. Crc Critical Reviews in Solid State and Materials Sciences 1983;11(2):123–87.
[27] Frisch HL., Diffusion of penetrants in polymers. journal of Polymer Science, Part C:Polymer Symposium, 1965.
[28] Frisch HL. Anomalous polymer-penentrant permeation. Journal of Chemical Physics 1962;37:2408–13.

[29] Vrentas JS, Vrentas CM. Differential sorption in glassy polymers. Journal of Applied Polymer Science 1999;71(9):1431–40.
[30] Vrentas JS, Duda JL, Huang WJ. Regions of fickian diffusion in polymer solvent systems. Macromolecules 1986;19(6):1718–24.
[31] Vrentas JS, Duda JL, Hou AC. Anomalous sorption in poly(ethyl methacrylate). Journal of Applied Polymer Science 1984;29(1):399–406.
[32] Crank J. The mathematics of diffusion. 2nd ed., New York: Oxford University Press; 1975.
[33] Hopfenberg HB, Stannett V. In: Haward RN, editor. The physics of the glassy state. London: Applied Science Publishers, Ltd; 1973.
[34] Tihminlioglu F, Danner RP, Lutzow N, Duda JL. Solvent diffusion in amorphous polymers: polyvinyl acetate–toluene system. Journal of Polymer Science, Part B:Polymer Physics 2000;38(18):2429–35.
[35] Wang BG, Yamaguchi T, Nakao SI. Solvent diffusion in amorphous glassy polymers. Journal of Polymer Science, Part B:Polymer Physics 2000;38(6):846–56.
[36] Lutzow N, Tihminlioglu A, Danner RP, Duda JL, De Haan A, Warnier G, et al. Diffusion of toluene and *n*-heptane in polyethylenes of different crystallinity. Polymer 1999;40(10):2797–803.
[37] Zimmerman CM, Singh A, Koros WJ. Diffusion in gas separation membrane materials: a comparison and analysis of experimental characterization techniques. Journal of Polymer Science, Part B:Polymer Physics 1998;36(10):1747–55.
[38] Bagley E, Long FA. 2-Stage sorption and desorption of organic vapors in cellulose acetate. Journal of the American Chemical Society 1955;77(8):2172–8.
[39] McDowell CC, Freeman BD, McNeely GW. Acetone sorption and uptake kinetic in poly(ethylene terephthalate). Polymer 1999;40(12):3487–99.